ELSEVIER

0958-9465(95)00030-5

Cement & Concrete Composites **18** (1996) 251–269

0958-9465/96/$15.00

Fracture Toughness of Micro-Fiber Reinforced Cement Composites

N. Banthia[a] & J. Sheng[b]

[a]Department of Civil Engineering, University of British Columbia, Vancouver, BC, V6T 1Z4, Canada
[b]Graduate Student, Department of Civil Engineering, Laval University, Ste-Foy, Quebec, G1K 7P4, Canada

Abstract

Toughness and strength improvements in cement-based matrices due to micro-fiber reinforcement were investigated. Cement paste and cement mortar matrices were reinforced at 1, 2 and 3% by volume of carbon, steel and polypropylene micro-fibers, and these composites were then characterized in the hardened state under an applied flexural load. Both notched and un-notched specimens were tested in four-point bending. Considerable strengthening, toughening and stiffening of the host matrix due to micro-fiber reinforcement was observed. The test data from the notched specimens was used to construct crack growth resistance and crack opening resistance curves for these composites and to identify the conditions necessary for failure. This paper recognizes the potential of these composites in various applications and stresses the need for continued research. © 1996 Elsevier Science Limited.

INTRODUCTION

The improvements in the mechanical properties of concrete due to fiber reinforcement are well known.[1] While conditions of unstable crack propagation are attained soon after its nucleation in an unreinforced cement-based matrix, cracks are bridged by fibers in a fiber reinforced composite such that the composite can carry a load well beyond matrix cracking. Fibers bridging crack faces restrict the cracks from widening and propagating and thus impart 'toughness' or energy absorption capability to the composite. Tensile strength of the composite, on the other hand, which is related more to the stress at which matrix develops a macrocrack, is not very different from the unreinforced matrix itself for most conventional fiber reinforced cement-based materials.

Lately, cement composites reinforced with a high volume fraction of fine, micro-fibers have been developed which are not only tougher but also stronger in tension than the parent matrix.[2] In order to indicate the fine size of these micro-fibers and also to distinguish them from the large macro-fibers, an arbitrary lower limit of 200 cm^2/g has been proposed as the specific surface area.[2] Given their fine size, in the composite, micro-fibers are able to provide reinforcing mechanisms at the micro-level such that the matrix cracks are arrested and stabilized before they acquire unstable dimensions. It has also been proposed that in the presence of micro-fibers, the intrinsic performance of the matrix itself is enhanced.[3,4] If the conditions are favorable, these composites can also depict pseudo-strain-hardening well beyond first cracking which is manifested as a nonlinear increase in stress beyond the 'Bend Over Point'[3] with an increase in the imposed deformations. This behavior of micro-fiber reinforced composites is very appealing from both mechanical and durability considerations.

While significant effort has been made in the past to characterize the engineering properties of micro-fiber reinforced composites, little effort has so far been made to study fracture in these composites.

CRACK GROWTH RESISTANCE IN FIBER REINFORCED CEMENT COMPOSITES

Most of our modern day understanding of crack propagation in brittle materials is due to Grif-

fith who in 1920 demonstrated that for an existing crack to grow in a linearly elastic, perfectly brittle material, a balance must exist between the increase in surface energy due to the propagation and the corresponding decrease in the potential energy of the system. In its modified form, the theory of Linear Elastic Fracture Mechanics (LEFM) states that a crack of length a in an infinite plate of ideally brittle material will propagate under an applied far-field stress, σ, when the following condition is satisfied:

$$K=K_c=\sigma\sqrt{(\pi a)} \quad (1)$$

where, K_c is called the fracture toughness which is believed to be a material property. Notice that the theory relates the apparent strength in tension to the dimension of the critical flaw in the material such that a new design criterion, K_c, emerges.

The above analysis, although applicable to perfectly brittle materials like glass, is not valid for ductile materials like metals and quasi-brittle materials like concrete. In the case of metals, a region of plasticity develops at the tip of a loaded crack where the stresses exceed the yield strength of the material. As an approximation, if the radius of the plastic zone stays small compared to the original length of the crack, the same can be accounted for by calculating the effective fracture toughness, K_{eff}, with the effective crack length assumed to be equal to the original crack length plus some fraction of the plastic zone radius.[5] Alternative to this equivalent elastic approach, one can reanalyze the problem of crack extension by imposing the closing pressure equal to the yield strength in the yielded portion of the crack as in Dugdale's Plastic Strip Model.[6] The equivalence of these two approaches has been demonstrated.[7]

In the case of concrete, considerable effort has also been made to study fracture using elastic and non-elastic fracture mechanics, and these have been extended to fiber reinforced concrete.[8] Analogous to the plastic zone in metals, a crack process zone is created at the tip of a crack[9] such that the crack propagates in a stable manner before it acquires critical dimensions needed for failure. However, while an estimation of the size of the process or yielded zone in metals is possible with reasonable accuracy, the same is not true in concrete; large variations are expected in the size of the process zone depending not only on the size and shape of the specimen but also on the loading conditions and the rate of loading. In addition. Plane stress conditions can be expected to pro-

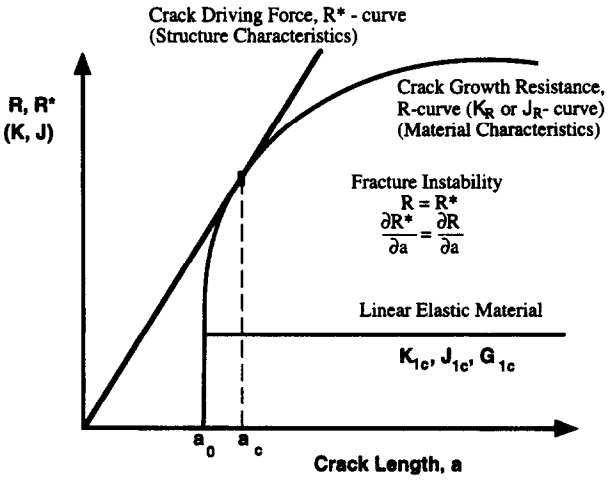

Fig. 1. Schematic of R-curve analysis.

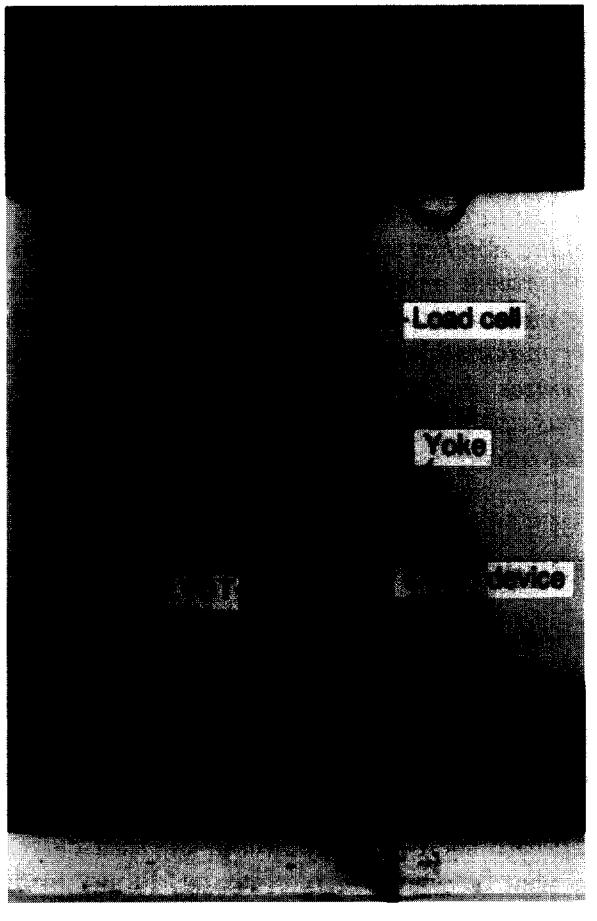

Fig. 2. A notched beam under third-point flexure. A yoke surrounding the specimen eliminates the spurious system deformations from the measured beam displacements. Sensors include an LVDT mounted under the beam to measure the vertical displacement and a clip-gauge to measure the crack mouth opening displacement (CMOD).

duce a process zone much larger than one produced under plane strain conditions. In spite of these difficulties, various ways of dealing with the nonlinear effects in fracture of concrete have been proposed. These include the cohesive crack models[10,11] and the effective crack models.[12] In the cohesive crack models, a closing pressure is introduced at the tip of a propagating crack to characterize fracture, and in the effective crack models, LEFM is applied to an equivalent elastic or an effective crack.

In fiber reinforced cement-based composites, along with the crack closing pressure due to aggregate interlocking in the matrix process zone ahead of a crack tip, fiber bridging occurs behind the crack tip to form what is commonly known as the fiber bridging zone. This makes the applications of traditional LEFM even more questionable to fiber reinforced composites. Hillerborg extended the cohesive crack model to fiber reinforced concrete and related the closing pressure to fiber and interfacial characteristics.[13] Closing pressure formulations in the fiber bridging zone were also developed by Visalvanich and Naaman[14] and by Wecharatana and Shah.[15]

Another elastic–plastic fracture criterion called the J-integral has been successfully applied to metals.[7] The J-integral[16] defines the stress conditions in the vicinity of a crack tip which can then be extended to those at the onset of critical propagation. Strictly speaking, therefore, J_c is a crack initiation — and not a crack propagation — criterion. This technique was adopted to characterize fiber reinforced concrete first by Mindess *et al.*[17] and later by Li *et al.*[18] who also obtained stress vs crack separation curves from the J-integral plots. Ohgishi and Ono[19] applied the analysis to polymer impregnated fiber reinforced mortars.

Finally, it is often argued that a single parameter description of fracture based on K_c, or J_c is not valid for cementitious materials and these materials in fact have an R-curve behavior.[20–23] An R-curve, in principle, is a crack growth resistance curve and it plots the K or J values at the tip of a crack as a function of crack extension or crack opening. Considered to be a

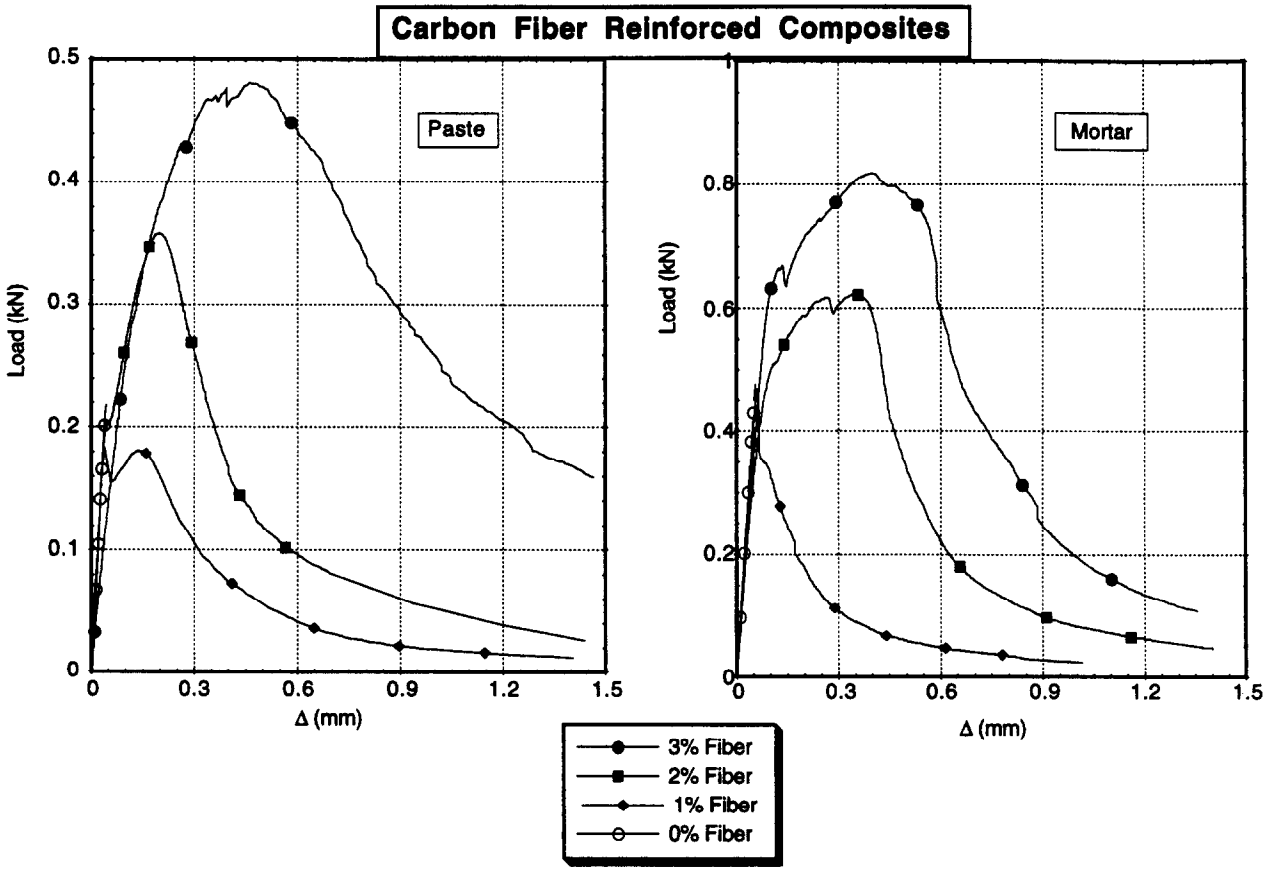

Fig. 3. Load–displacement plots for carbon fiber reinforced composites beams without a notch; (a) paste matrix, and (b) mortar matrix.

material property, an R-curve can be used to establish the conditions of fracture for a given specimen geometry and loading configuration.[24] The principles of R-curve analysis are shown in Fig. 1.

This paper examines fracture in micro-fiber reinforced cement composites based on the various available techniques of characterization.

EXPERIMENTAL PROGRAM

Materials and mixes

Two base matrices of cement paste (water : cement : silica fume = 0·35 : 1·00 : 0·20) and cement mortar (water : cement : silica fume : sand = 0·35 : 1·00 : 0·20 : 0·50) were reinforced with micro-fibers of carbon, steel and polypropylene at volume fractions of 1, 2 and 3%. Silica fume was used in all mixes for an effective dispersion of fibers.[25,26] Mechanical properties and geometrical characteristics of fibers were as follows (E is the elastic modulus and TS is the tensile strength):

Carbon fiber: 18 μm diameter, 6 mm long, E=30 GPa, TS=590 MPa
Steel fiber: 25 μm × 5 μm section, 3 mm long, E=200 GPa, TS=600 MPa
Polypropylene fiber: 4 μm diameter, 6 mm long, E=1·41 GPa, TS=32 MPa.

Presumably, the fibers had varyingly different surface characteristics and developed different interfacial bond strengths with the matrix.

Specimens and tests

Flexural specimens (25 mm × 25 mm × 225 mm) were cast using plexiglass moulds. One half of the specimens were left un-notched and in the other half of the specimens an 8 mm notch was cut using a fine saw. Both notched and un-notched specimens were tested in four-point bending with loading at the third-points. A

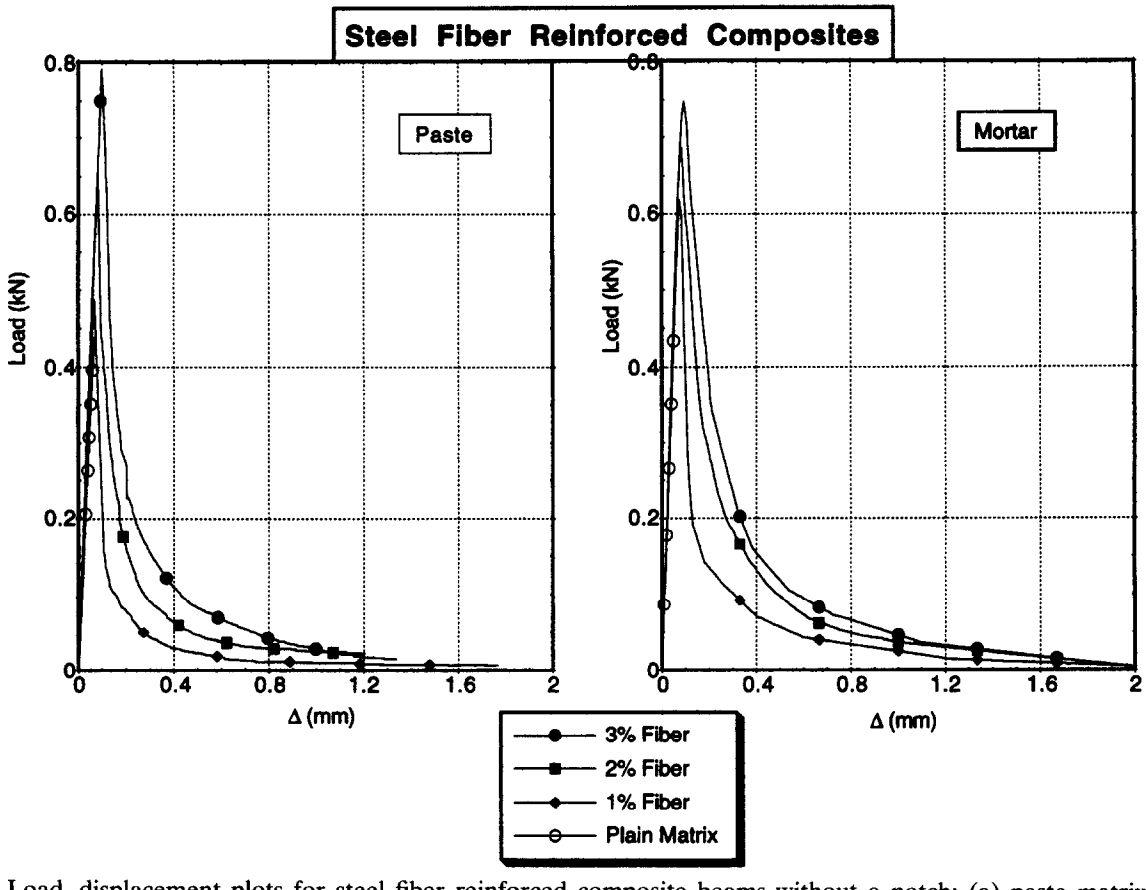

Fig. 4. Load–displacement plots for steel fiber reinforced composite beams without a notch; (a) paste matrix, and (b) mortar matrix.

notched specimen during test is shown in Fig. 2. Notice that a yoke is mounted around the specimen to eliminate spurious deformations arising due to support settlements during a test. It has been shown previously that the use of a yoke is necessary to measure deflections comparable with the theoretical values.[27] In the un-notched specimens, beam displacements at the center of the specimen were monitored by placing an LVDT in contact with the top of the specimen. For the notched specimens, in addition to beam center-point displacements, crack mouth opening displacements (CMOD) were also monitored by placing an extensometer across the notch using grips installed on either side of the notch. Load was applied at a cross-arm speed of 0·01 mm/min for the plain specimens and at a rate of 0·02 mm/min for the fiber reinforced specimens so as to terminate the test in a reasonable amount of time. The data from the two extensometers and the load cell were acquired electronically using a data-logger running at 10 Hz.

Data analysis

The data comprised of the applied load and the mid-span beam displacement plots for the unnotched beams, and the load vs mid-span displacement and load vs crack mouth opening displacement (CMOD) plots for the notched beams. While the applied load vs beam mid-span displacement plots for the un-notched beams were analyzed in a routine manner for strengths, fracture energies, etc., the load vs mid-span displacement plots and load vs CMOD plots acquired for notched specimens were analyzed as given in the Appendix.

RESULTS AND DISCUSSION

Un-notched beams

The load displacement curves for un-notched beams are given in Figs 3, 4 and 5, respectively, for carbon, steel and polypropylene fiber rein-

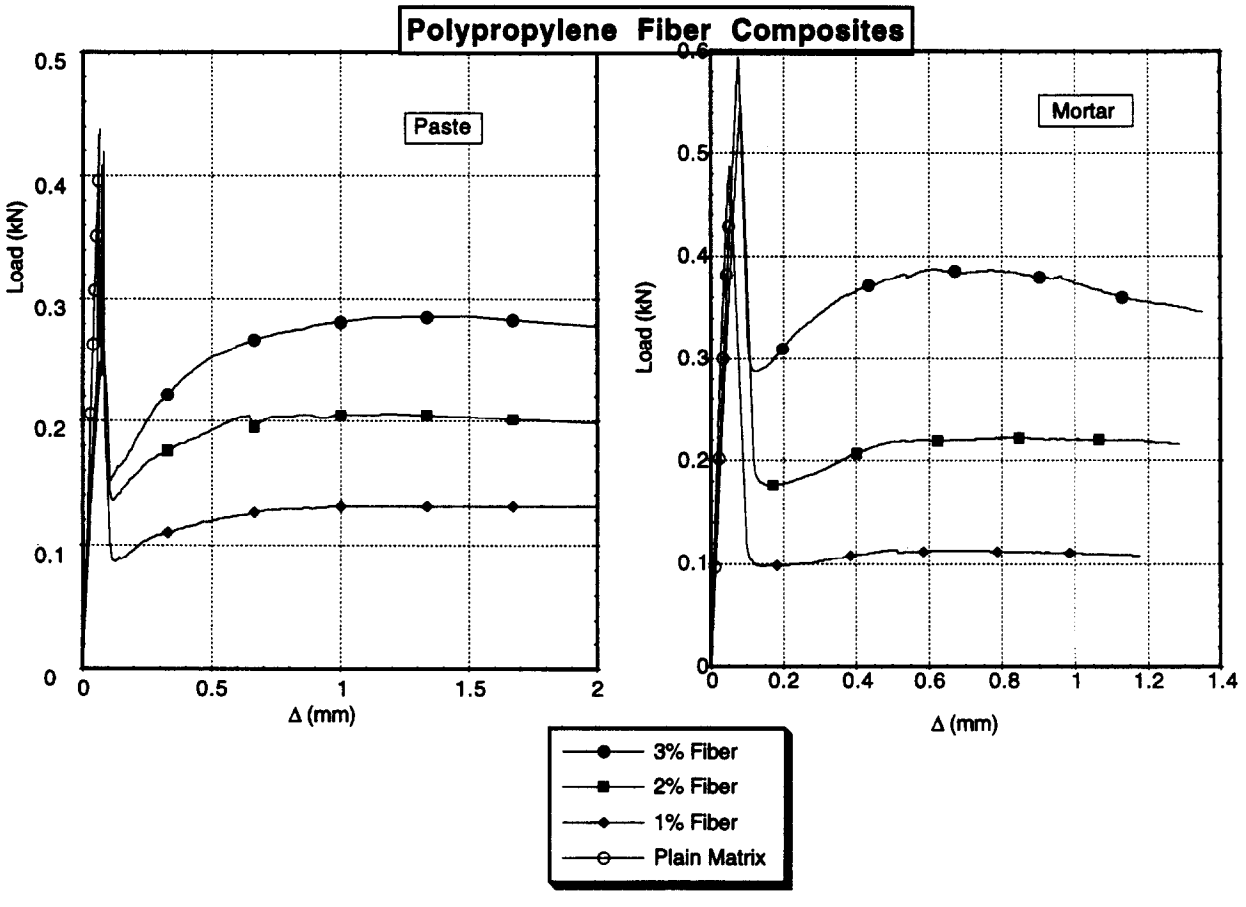

Fig. 5. Load–displacement plots for polypropylene fiber reinforced composite beams without a notch; (a) paste matrix, and (b) mortar matrix.

forced composites. These curves were analyzed to obtain the load and displacement at the Bend Over Point (i.e. the point at which first non-linearity in the load–displacement curve occurs), load and displacement at the ultimate load and the total fracture energy to a displacement of 2·5 mm. The use of the yoke around the specimens as reported before[27] allowed an accurate estimation of the displacements and hence permitted the calculation of the elastic modulus from the initial (linear) part of the curve. Ignoring shear deformations in the beam, the load and displacement values at the bend over point may be used to calculate the elastic moduli using the following equation:

$$\Delta = \frac{23PS^3}{1296EI} \tag{2}$$

where, Δ, is the beam mid-span displacement, P is the applied load, S is the span and EI is the flexural rigidity.

Flexural strength (modulus of rupture) values were calculated from the ultimate loads using simple elastic analysis. It is recognized that such an approach is not entirely valid given the non-linear nature of these curves. The results of tests on un-notched beams are given in Table 1.

Notice that in carbon–cement composites, an increase in fiber content led not only to an increase in the load carrying capacity but also to significant increases in the deformability or toughness. Steel fiber reinforcement also led to an improvement in the strength of the matrix, but the toughness improvements were not as pronounced as the carbon–cement composites. Finally, the presence of polypropylene fibers resulted in no increase in the strength but the post-peak load carrying capacity, hence the toughness, was improved. Improvements noticed above are also seen to be proportional to the fiber volume fraction. Similar behavior was observed in the case of composites tested in uni-axial tension.[2] There was no particular difference observed in the behavior of the

Table 1. Results from tests on un-notched beams

	*At BOP**			*At peak*			*Strength*		
Composite	*Load (N)*	*Displacement (mm)*	*E*** *(GPa)*	*Load (N)*	*Displacement (mm)*	*Total fracture energy (N-m)*	*Flexural (MPa)*	*Tensile**** *(MPa)*	*Ratio Flexural/ tensile*
PO	438	0·064	29·84	438	0·064	0·0145	5·60	2·96	1·89
PC1	456	0·067	29·67	486	0·126	0·1504	6·22	4·10	1·51
PC2	505	0·076	28·97	702	0·287	0·3348	8·98	6·10	1·47
PC3	625	0·071	38·38	718	0·377	0·5544	9·19	6·56	1·40
PS1	477	0·067	31·04	488	0·067	0·0672	6·24	4·40	1·41
PS2	639	0·082	33·97	649	0·081	0·1230	8·30	6·20	1·33
PS3	769	0·098	34·21	791	0·098	0·2040	10·12	7·32	1·38
PP1	458	0·065	30·72	458	0·065	0·2542	5·86	3·40	1·72
PP2	466	0·074	27·45	456	0·074	0·3882	5·83	3·55	1·64
PP3	482	0·086	24·43	464	0·086	0·5200	5·93	3·50	1·69
MO	475	0·065	31·86	475	0·065	0·0157	6·08	3·44	1·76
MC1	457	0·060	33·20	467	0·061	0·1307	5·97	4·75	1·25
MC2	500	0·097	22·47	622	0·347	0·3834	7·96	6·44	1·23
MC3	629	0·097	28·27	818	0·400	0·6418	10·47	7·10	1·47
MS1	617	0·074	35·91	641	0·080	0·1182	8·20	6·10	1·34
MS2	686	0·082	36·29	714	0·083	0·1861	9·13	7·21	1·26
MS3	748	0·097	33·97	750	0·094	0·2357	9·60	7·79	1·23
MP1	468	0·052	40·59	487	0·052	0·2349	6·23	4·20	1·48
MP2	524	0·062	36·84	546	0·063	0·4384	6·98	4·25	1·64
MP3	554	0·076	31·78	577	0·078	0·7250	7·38	4·35	1·69

*Bend over point.
**From

$\Delta = \frac{23PS^3}{1296EI}$ (ignoring shear) at BOP.

***From Ref. 2.

composites based on the mortar matrix than those based on the paste matrix. Flexural strengths for the various composites, as expected, were higher than their tensile strengths and the strength ratios (flexural/tensile) follow the trends usually reported by others.[28]

The elastic moduli calculated from the load

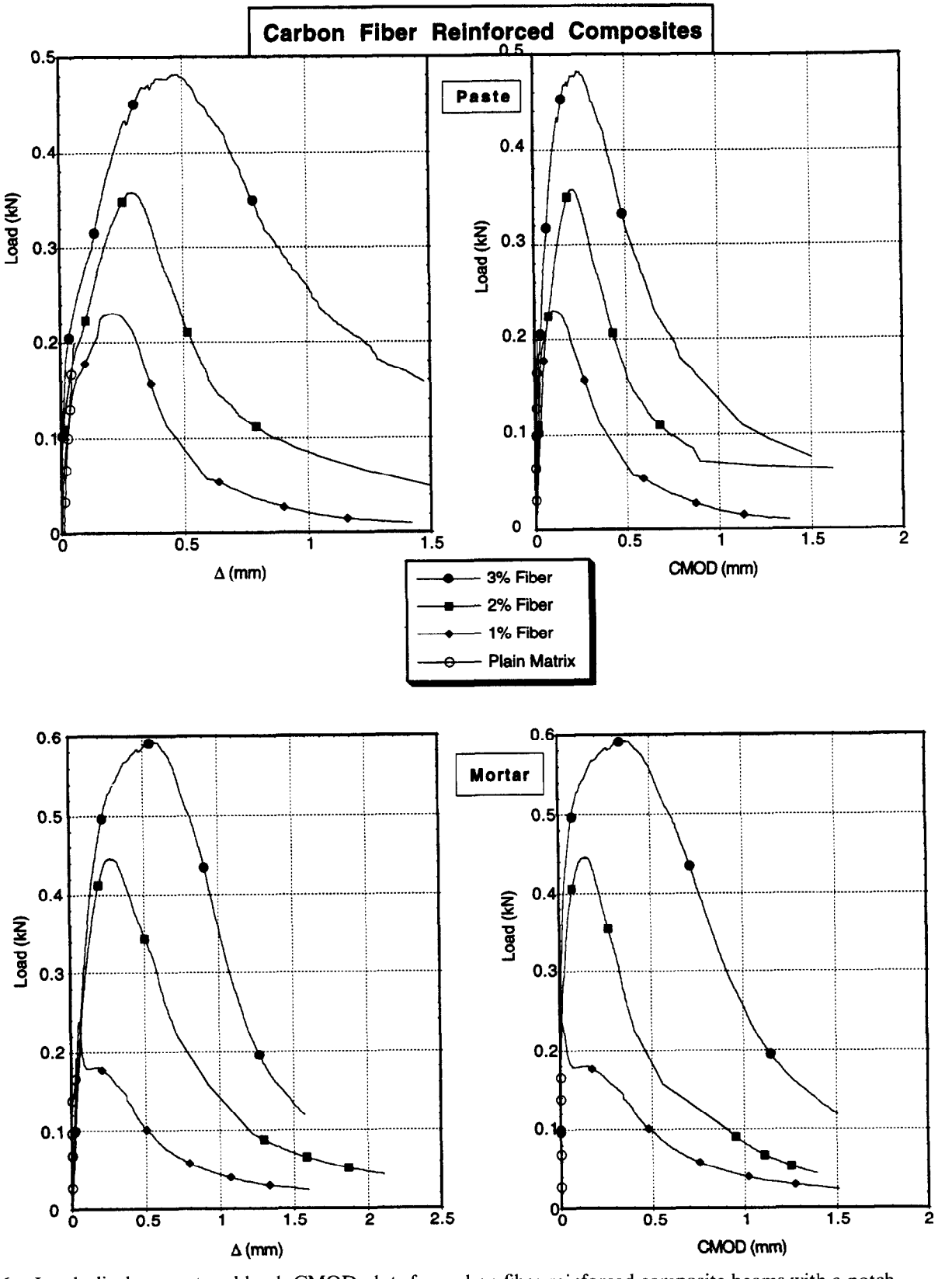

Fig. 6. Load–displacement and load–CMOD plots for carbon fiber reinforced composite beams with a notch.

and displacement values at the BOP (eqn (2)) and reported in Table 1, fail to indicate any particular trend. Part of the reason is the general uncertainty regarding the exact location of BOP which is often subject to human judgement errors.

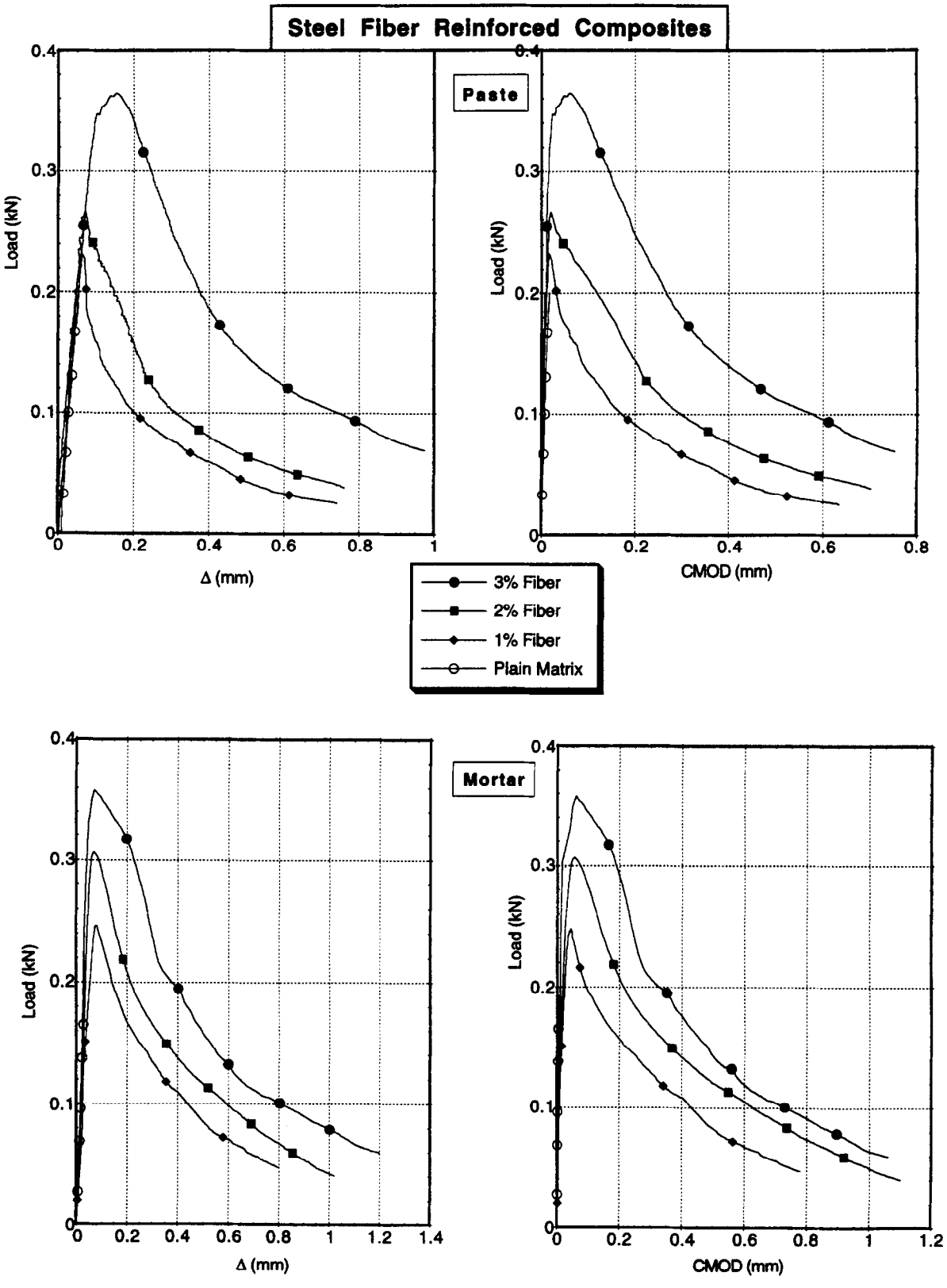

Fig. 7. Load–displacement and load–CMOD plots for steel fiber reinforced composite beams with a notch.

Notched beams

Experimental curves for the notched beams are given in Figs 6, 7 and 8. In these figures, applied load vs the beam mid-span displacement and applied load vs the crack mouth opening displacement (CMOD) plots are shown for carbon, steel and polypropylene fiber rein-

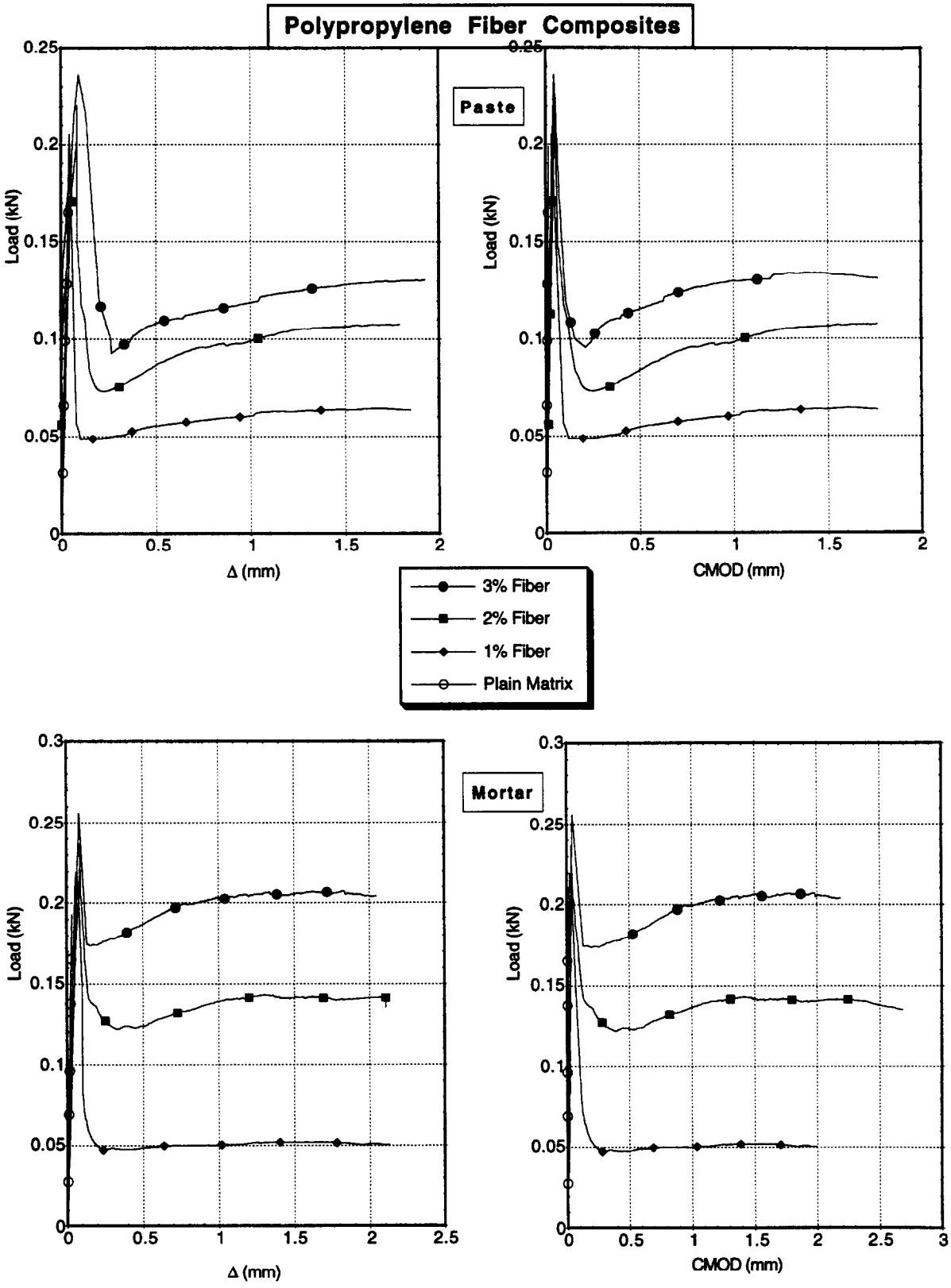

Fig. 8. Load–displacement and load–CMOD plots for polypropylene fiber reinforced composite beams with a notch.

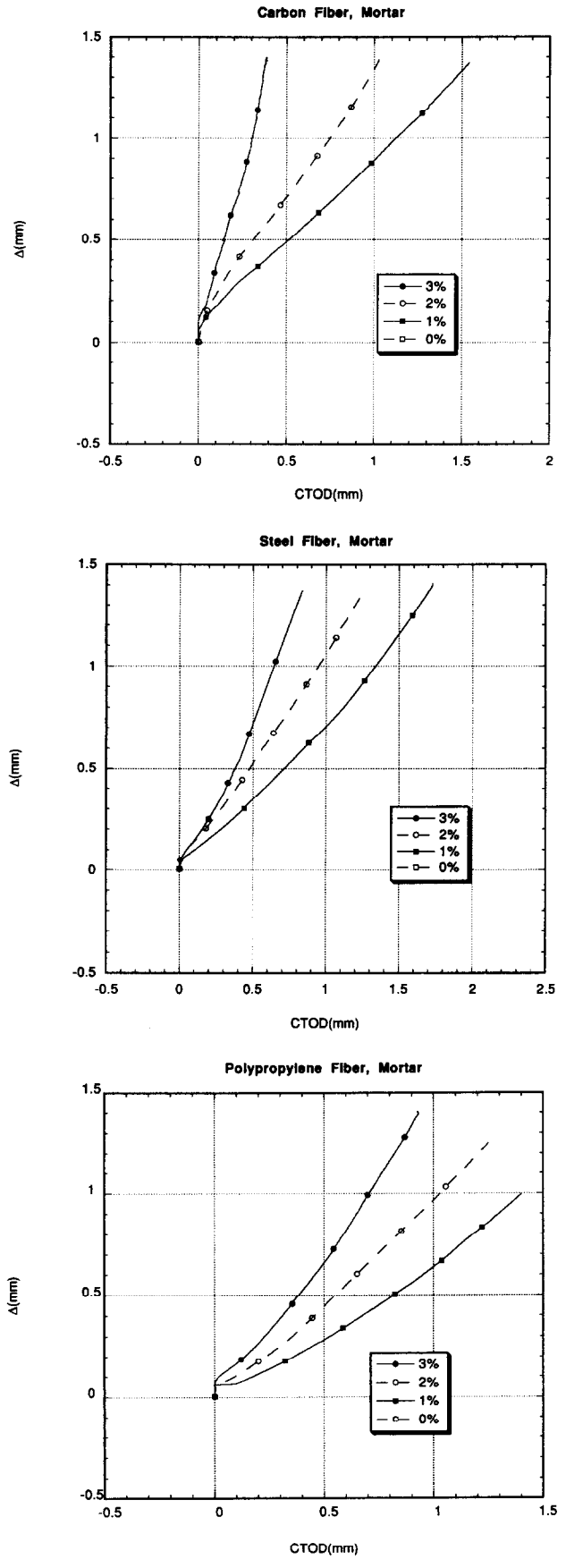

Fig. 9. Vertical displacements Δ plotted as a function of the CTOD for the notched beams; (a) carbon fiber reinforced composites, (b) steel fiber reinforced composites, and (c) polypropylene fiber reinforced composites.

forced composites based on paste and mortar matrices. In Figs 9(a), (b) and (c), some plots of beam vertical displacement (Δ) are plotted against crack tip opening displacements, CTOD for carbon, steel and polypropylene fiber reinforced mortars, respectively. Notice that as the fiber volume fraction is increased, there is a decrease in the CTOD values at a given beam displacement. This is a direct indication of the more effective crack bridging rendered by fibers when present in the composite at a higher volume fraction. Note also that the CTOD values at a given fiber volume fraction are greater for polypropylene fiber reinforced composite than those reinforced with steel or carbon fibers. This may be a direct consequence of the lower modulus of elasticity of polypropylene fibers than carbon or steel fibers and also indicative of the poor bond developed in their case.

The data for the notched beams were analyzed and the results are given in Table 2. In particular, the following conditions at the peak load are reported: the load, the displacement, CMOD, CTOD, fracture toughness based on initial crack length (K_{I,a_o}), the effective crack length, a_{eff}, obtained using compliance calibration, and the fracture toughness based on the effective crack length ($K_{I,a_{eff}}$). Also given in Table 2 are the Notch Sensitivity Factors defined as the ratio of peak load supported by a notched beam to that supported by an un-notched beam of the same material. As expected, notched beams supported reduced ultimate loads and this reduction was more pronounced for steel and polypropylene fiber reinforced composites as compared to carbon fiber reinforced composites. This is related to the superior fracture toughness of carbon fiber reinforced composites as discussed later. Notice also that while the curves for the notched beams have, in general, shapes similar to those for the un-notched beams, the brittleness observed in steel fiber reinforced un-notched beams is not as pronounced in the notched beams. Fracture toughness values based on the initial length of the crack (a_o), K_{I,a_o}, indicate the superior fracture toughness of carbon and steel micro-fiber reinforced composites. However, based on fracture toughness values calculated using the modified crack lengths (a_{eff}), $K_{I,a_{eff}}$, the very high fracture toughness of carbon fiber reinforced mortars over all other composites becomes noticeable.

Table 2. Results from tests on notched beams

	Conditions at the peak load								*Conditions at unstable fracture (from K_R curves)*		
Composite	*P (N)*	*NSF*	*Δ (mm)*	*CMOD (mm)*	*†CTOD (mm)*	**K_{I,a_o} (mPa$\sqrt{m}$)*	***a_{eff} (mm)*	****$K_{I,a_{eff}}$ (mPa$\sqrt{m}$)*	*K_{IC} (mPa$\sqrt{m}$)*	*$CTOD_c$ (mm)*	*$CMOD_c$ (mm)*
PO	199	0·45	0·0248	0·0167	0·0003	0·46	8·00	0·46	0·46	0·0003	0·0167
PC1	230	0·50	0·2130	0·1027	0·0334	0·53	9·43	0·62	0·92	0·1786	0·3034
PC2	358	0·70	0·2940	0·2093	0·1006	0·83	12·06	1·29	1·54	0·2112	0·3652
PC3	482	0·77	0·4610	0·2413	0·1202	1·12	12·55	1·84	2·33	0·3478	0·5722
PS1	232	0·48	0·0350	0·0170	0·0047	0·54	8·96	0·59	1·32	0·0862	0·1371
PS2	266	0·41	0·0720	0·0199	0·0058	0·62	9·08	0·69	1·78	0·1018	0·1633
PS3	364	0·47	0·0850	0·0605	0·0322	0·84	13·70	1·61	2·62	0·1412	0·2245
PP1	205	0·44	0·0450	0·0338	0·0052	0·47	8·27	0·40	0·47	0·0052	0·0338
PP2	220	0·47	0·0840	0·0466	0·0062	0·51	8·35	0·51	0·51	0·0062	0·0466
PP3	236	0·48	0·0930	0·0449	0·0065	0·54	8·44	0·55	0·54	0·0065	0·0449
MO	192	0·40	0·0360	0·0194	0·0005	0·45	8·03	0·45	0·45	0·0005	0·0194
MC1	238	0·52	0·0560	0·0117	0·0038	0·55	9·37	0·64	2·46	0·1849	0·2863
MC2	455	0·91	0·2750	0·1455	0·0830	1·06	15·94	2·72	3·40	0·1874	0·3007
MC3	591	0·93	0·5760	0·3326	0·2007	1·37	17·55	4·67	5·70	0·3867	0·6148
MS1	247	0·40	0·0420	0·0428	0·0144	0·57	9·55	0·67	1·45	0·1995	0·3166
MS2	306	0·44	0·0720	0·0500	0·0195	0·71	10·25	0·90	1·80	0·2218	0·3850
MS3	356	0·47	0·0800	0·0600	0·0314	0·83	13·39	1·40	2·74	0·3167	0·2211
MP1	219	0·46	0·0660	0·0269	0·0082	0·51	8·42	0·55	0·51	0·0082	0·0269
MP2	236	0·45	0·0830	0·0346	0·0147	0·55	9·16	0·55	0·55	0·0147	0·0346
MP3	255	0·46	0·0900	0·0452	0·0165	0·59	9·36	0·59	0·59	0·0165	0·0452

NSF; notch sensitivity factor=$[(P_{max})_{notched}]/[(P_{max})_{unnotched}]$.
*Based on initial crack length a_o.
**Calculated from compliance calibration.
***Based on effective crack length, a_{eff}, at the peak load.
†Calculated from CMOD.

It is often argued that a single parameter representation of fracture in cement-based materials is not valid. Instead, therefore, a crack growth resistance curve (R-curve) is preferred where the crack growth resistance expressed as the stress intensity factor, K, at the tip of a crack is plotted as a function of crack extension. It is proposed that such an R-curve may be used as a measure of toughening provided by the fibers and also treated as a material property (Fig. 1). In Figs 10, 11 and 12 Crack Growth Resistance Curves (CGRC) are given for carbon, steel and polypropylene fiber reinforced composites. Notice that for carbon and steel fiber reinforced composites, the peak value of K occurs not at the peak load but after the peak load. In Table 2 the peak value of K regardless of where it is on the R-curve is noted as K_{IC} (the true fracture toughness), and the corresponding crack tip and crack mouth displacements, $CTOD_c$ and $CMOD_c$, are also noted. The higher values of K_{IC}, $CTOD_c$ and $CMOD_c$ for the carbon fiber reinforced composites than other composites indicate, once again, the significantly high fracture resistance of these composites. It is worth noticing that the engineering properties obtained in a conventional manner using un-notched beams (Table 1) fail to recognize this important feature of carbon fiber reinforced composites.

The K_R-curves in Figs 10, 11 and 12 were plotted as a function of a_{eff} obtained from the compliance calibration. However, as shown in Fig. 13, a crack rarely takes a straight path and the tortuous path taken as the crack diminishes brings into question the validity of this type of analysis. Alternatively, one can replot the stress intensity factors at the crack tip as a function of the crack tip opening displacement (CTOD) instead of the effective crack length. In this regard, it is believed that while the applied load and the effective crack length rapidly approach a limiting value during a test, crack opening displacement values approach failure conditions in a relatively stable manner.[7] Based on these reasons, one can argue that plots of K_{eff} vs CTOD may be a more reasonable way of characterizing these composites. Such curves, termed the Crack Opening Resistance Curves (CORC) are also shown in Figs 10, 11 and 12. Clearly, the calculation of K_{eff} still involves esti-

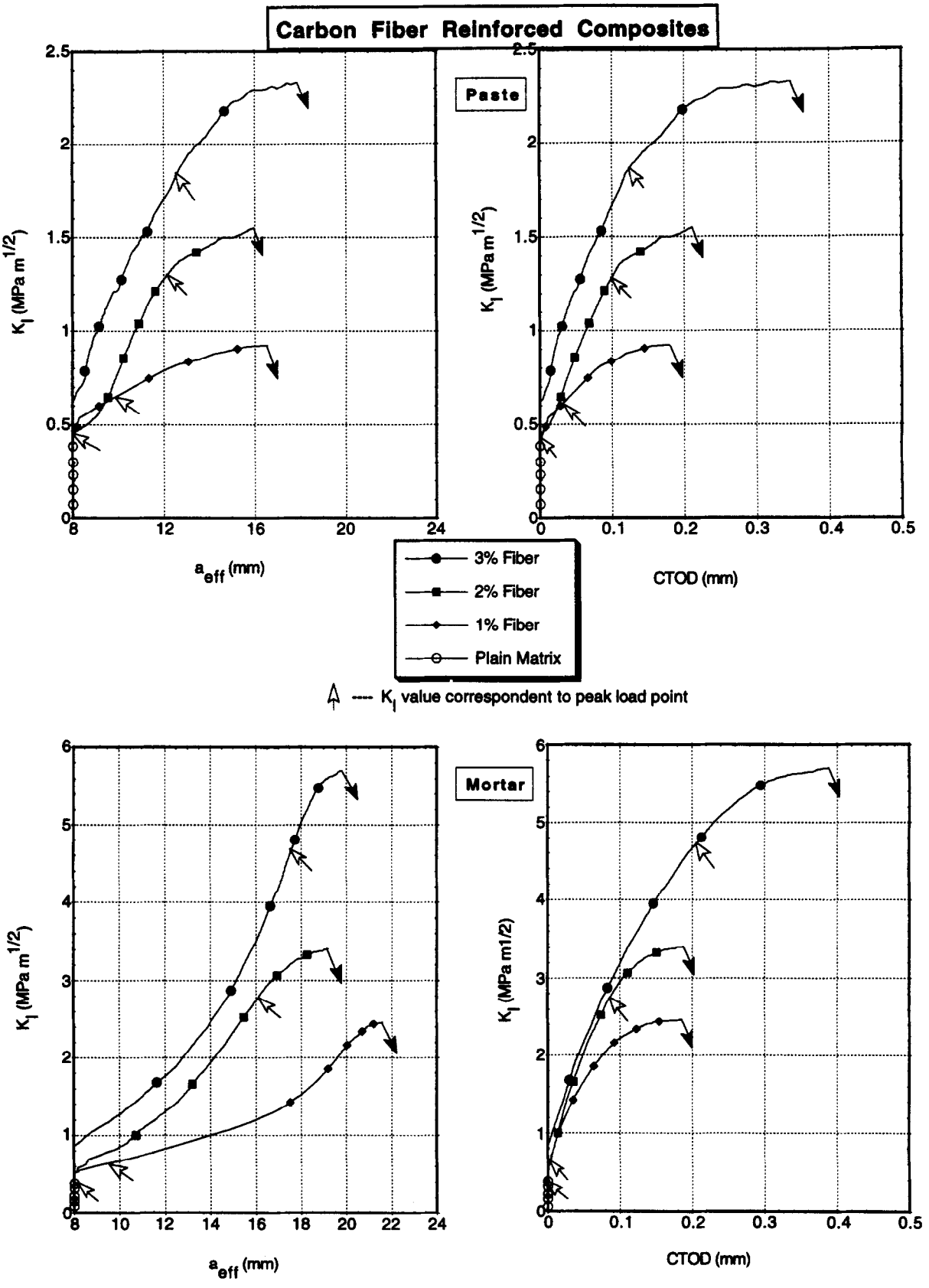

Fig. 10. K_R-curves for carbon fiber reinforced composites plotted as crack growth resistance (K_I vs a_{eff}) and crack opening resistance (K_I vs CTOD) curves.

mating a_{eff} from compliance calibration such that K_{eff} carries all the inaccuracies of this type

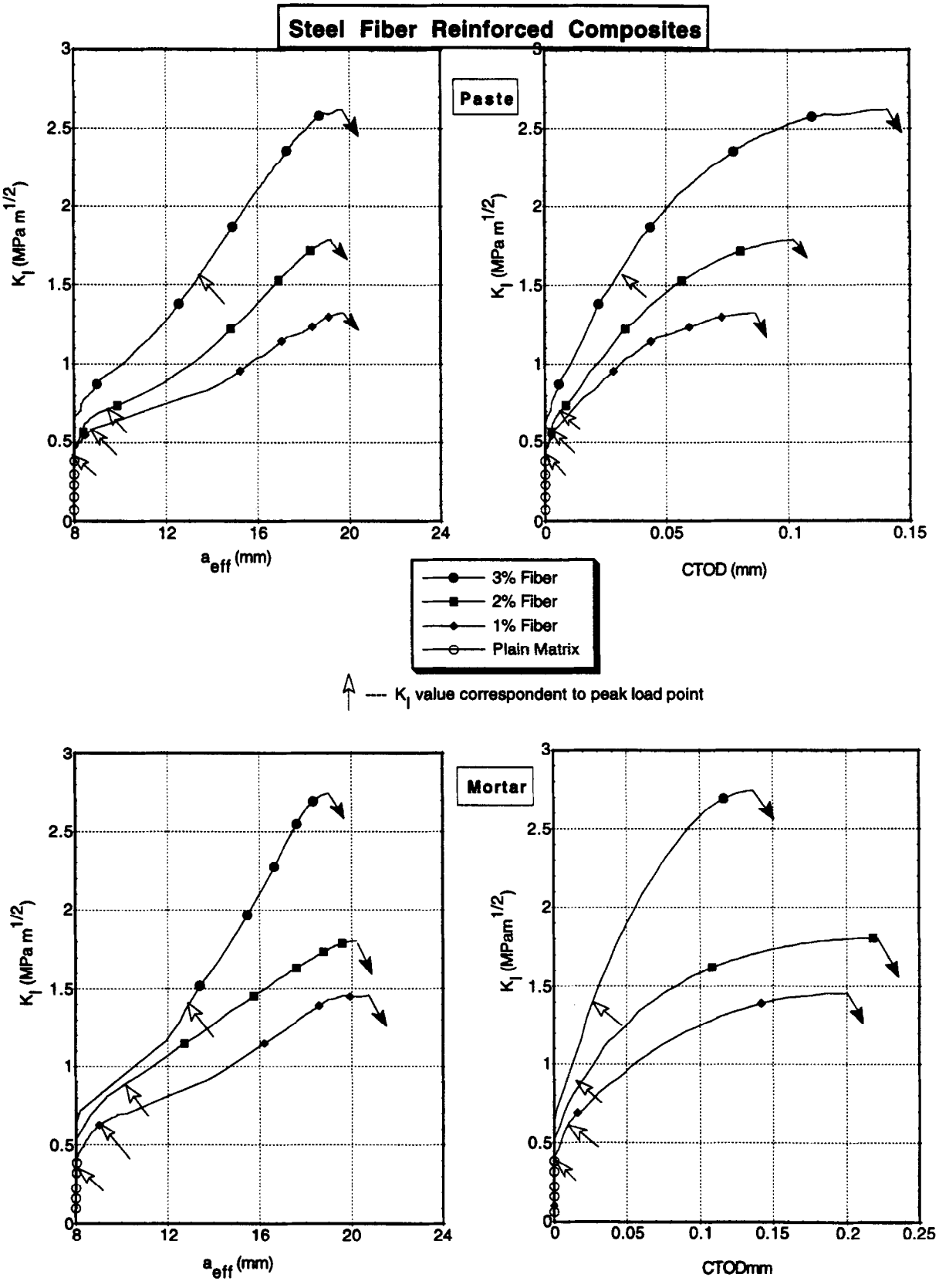

Fig. 11. K_R-curves for steel fiber reinforced composites plotted as crack growth resistance (K_I vs a_{eff}) and crack opening resistance (K_I vs CTOD) curves.

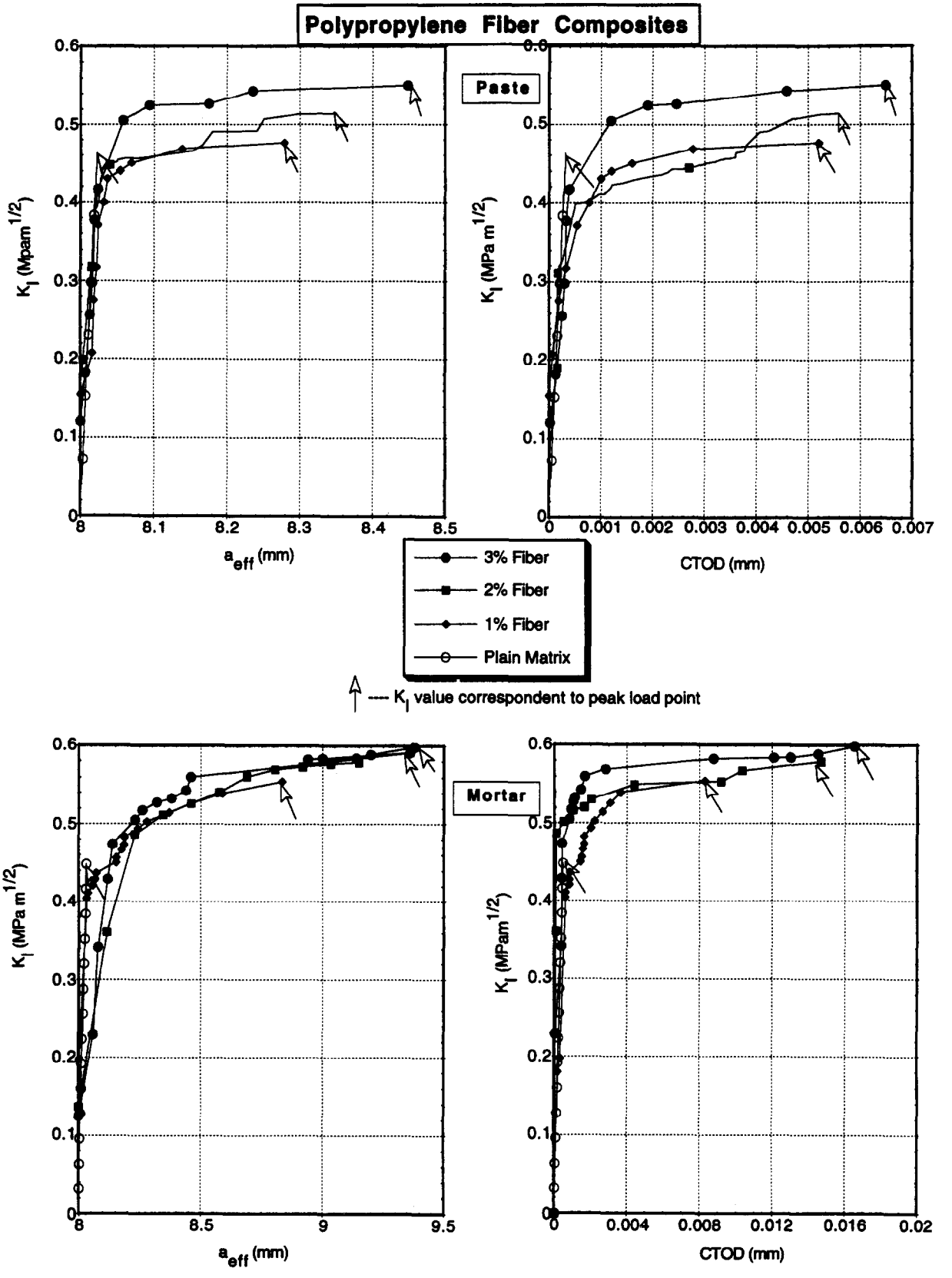

Fig. 12. K_R-curves for steel fiber reinforced composites plotted as crack growth resistance (K_I vs a_{eff}) and crack opening resistance (K_I vs CTOD) curves.

of analysis and the peak value of K_{eff} in the Crack Opening Resistance Curves is not any different from that in the Crack Growth Resistance Curves.

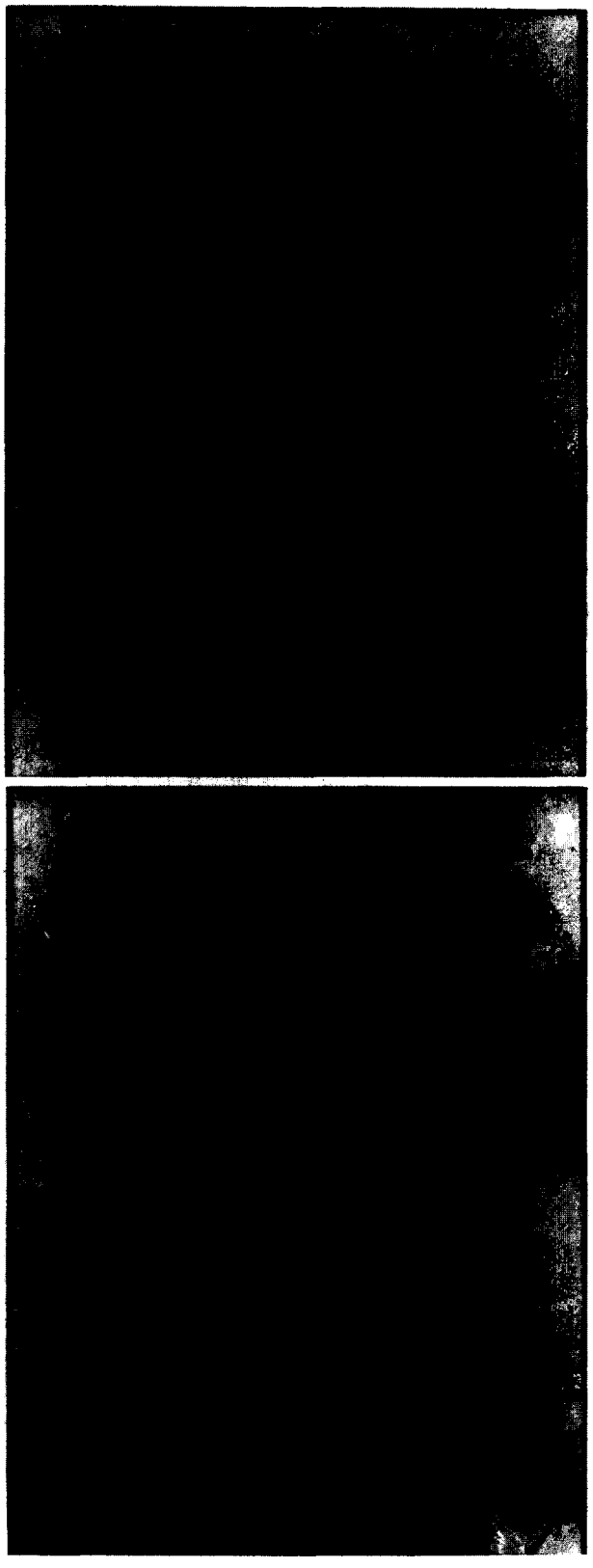

Fig. 13. Micrograph showing the tortuous path taken by a crack in polypropylene fiber reinforced composite.

One additional outcome of the Crack Opening Resistance Plots is the critical value of the crack tip opening displacement, $CTOD_c$, occurring at the peak value of K_{eff}, which in itself can be treated as a fracture criterion. These values are noted in Table 2 along with the corresponding values of the $CMOD_c$ for the various composites. It is to be recognized, however, that the values of $CTOD_c$ reported in Table 2 are a function of the specimen geometry and not a fundamental property of the composites.[7] Also, $CTOD_c$ values for the various composites are not only a function of the fiber length but also of the strength of the interfacial bond.

APPLICATIONS OF MICRO-FIBER REINFORCED COMPOSITES

Micro-fiber reinforced cement-based composites, especially the ones with a high fracture toughness, are potentially useful in thin precast products like roofing sheets, tiles, curtain walls, cladding panels, I- and L-shaped beams, permanent forms, etc. They may also prove significantly useful as a material for thin repairs and patching. Some of these composites can be good conductors of electricity which makes them a candidate for static free floors, lightning arresters, etc. Their full potential, however, may not be realized until they are optimized from the strength and toughness considerations and their physical properties, volume stability, durability and other relevant properties are fully assessed. Some such data is now available.[29–31]

CONCLUDING REMARKS

This paper examines the improvements in the fracture toughness of cement-based materials reinforced with a high volume fraction of carbon, steel and polypropylene micro-fibers. Tests on notched and un-notched beams were conducted which led not only to the engineering properties but also to Crack Growth Resistance Curves and Crack Opening Resistance Curves plotted in terms of the stress intensity factor, K at the crack tip. These K_R-curves, indicate the exceptionally high fracture toughness of carbon fiber reinforced composites over the other composites and provide a valuable insight into the toughening mechanisms that exist in these composites. Significant research is still needed,

however, to identify the experimental factors which influence the curve itself and to model the curve in terms of fiber, matrix and interfacial properties.

ACKNOWLEDGEMENTS

The continued support of the Natural Sciences and Engineering Research Council of Canada is gratefully acknowledged. Thanks are also due to Novocon International, Fibrin, Inc., and Kreha Corporation of America for supplying the fibers.

REFERENCES

1. Barr, B. I. G., Fiber Reinforced Concrete: Where Do We Go From Here? In *Fiber Reinforced Cement and Concrete*. ed. R. N. Swamy, Proceedings RILEM Symposium. E. & F. N. Spon, 1992, pp. 3–11.
2. Banthia, N., *et al.*, Uni-axial Tensile Response of Micro-Fiber Reinforced Cement Composites, RILEM, *Materials and Structures*, to appear.
3. Ouyang, C. & Shah, S. P., Toughening of high strength cementitious matrix reinforced by discontinuous short fibers. *Cement and Concrete Research*, **22** (1992) 1201–15.
4. Beaudoin, J. J., Microstructural Modifications of Macro and Micro-Fiber Reinforced Hydrated Portland Cement Matrices, In *Proc. 1st Can. University-Industry Workshop on Fiber Reinforced Concrete*, ed. N. Banthia, Quebec City, 1991, pp. 129–39.
5. Irwin, G. R., *Handbuch der Physik*, Vol VI. Springer, Berlin, 1958, p. 551.
6. Dugdale, D. S., *Journal of Mechanics and Physics of Solids*, **8** (1960) 100.
7. Hertzberg, R. W., *Deformation and Fracture Mechanics of Engineering Materials*. John Wiley and Sons, New York, 1976.
8. Swamy, R. N., Fracture Mechanics Applied to Concrete, In *Developments in Concrete Technology — 1*, ed. F. D Lydon. Applied Science Publishers Ltd, 1979, pp. 221–81.
9. Mindess, S., The Fracture Process Zone in Concrete, In *Toughening Mechanisms in Quasi-Brittle Materials*, ed. S. P. Shah. Kluwer Academic Publishers, The Netherlands, pp. 271–86.
10. Hillerborg, A., Modeer, M. & Peterson, P.-E., Analysis of crack formation and crack growth in concrete by means of fracture mechanics and finite elements. *Cement and Concrete Research*, **6** (1976) 773–82.
11. Bazant, Z. P. & Oh, B. H., Crack band theory for fracture of concrete. *Materials and Structures*, **16**(83) (1983) 155–77.
12. Jenq, Y. S. & Shah, S. P., Two parameter fracture model for concrete. *ASCE Journal of Engineering Mechanics Division*, **111**(10) (1985) 1227–41.
13. Hillerborg, A., Analysis of fracture by means of the fictitious crack model, particularly for fiber reinforced concrete. *Journal of Cement Composites and Lightweight Concrete*, **2** (1980) 177–84.
14. Wecharatana M. & Shah, S. P., A model for predicting fracture resistance of fiber reinforced concrete. *Cement and Concrete Research*, **13** (1983) 819–29.
15. Visalvanich, K. & Naaman, A. E., Fracture model for fiber reinforced concrete. *ACI Journal*, **March–April**, (1983) 128–38.
16. Rice, J. R., Paris, P. C. & Merkle, J. G., *Progress in Flaw Growth and Fracture Toughness Testing, ASTM STP 536*. American Society for Testing and Materials, 1973, pp. 231–45.
17. Mindess, S. Lawrence, F. W. & Kesler, C. E., The J-integral as a fracture criterion for fiber reinforced concrete. *Cement and Concrete Research*, **7** (1977) 731–42.
18. Li, Victor C., Chan, Chun-Man & Leung, Christopher K. Y., Experimental determination of the tension-softening relations for cementitious composites. *Cement and Concrete Research*, **17** (1987) 441–52.
19. Ohgishi, S. & Ono, H., Non-linear Fracture Toughness (J_{IC}, G_F) of Inorganic Polymer Impregnated Cement Mortar Reinforced by New Material Fiber, In *Fracture of Concrete and Rock: Recent Developments*, eds S. P. Shah, S. E. Swartz & B. Barr. Elsevier Applied Science, 1989, pp. 71–80.
20. Visalvanich, Kitisak & Naaman, Antoine E., Fracture methods in cement composites. *ASCE Journal of Engineering Mechanics Division*, **107**(EM6) (1981) 1155–71.
21. Mai, Yiu-Ming, Failure Characterization of Fiber Reinforced Cement Composites with R-Curve Characteristics, In *Toughening Mechanisms in Quasi-Brittle Materials*, ed. S. P. Shah. Kluwer Academic Publishers, The Netherlands, 1991, pp. 467–505.
22. Karihaloo, B. L., Do Plain and Fiber Reinforced Concretes have an R-Curve Behavior? *SEM-RILEM Int. Conf. on Fracture of Concrete and Rock*, Houston, Texas, 1987, pp. 128–37.
23. Mobasher, B., Ouyang, C. & Shah, S. P., Modeling of fiber toughening in cementitious materials using an R-curve approach. *International Journal of Fracture*, **50** (1991) 199–219.
24. McCabe, D. E. (ed.), *Fracture Toughness Evaluation by R-Curve Methods, ASTM-STP 527*. American Society for Testing and Materials, Philadelphia, PA, 1973, 112 pp.
25. Banthia, N., Pitch-based carbon fiber reinforced cements: structure, performance, applications and research needs. *Canadian Journal of Civil Engineering*, **19** (1992) 26–38.
26. Ohama, Y., Carbon–cement composites. *Carbon*, **27**(5) (1989) 729–37.
27. Banthia, N. & Trottier, J.-F., Test methods for flexural toughness characterization of fiber reinforced concrete: some concerns and a proposition. *ACI Materials Journal*, in press, 1994.
28. Wright, P. J. F., Comment on an indirect tensile test on concrete cylinders. *Magazine of Concrete Research (London)*, **7**(20) July (1955) 87–96.
29. Banthia, N., Djeridane, S. & Pigeon, M., Electrical resistivity of cements reinforced with micro-fibers of carbon and steel. *Cement and Concrete Research*, **22**(5) (1992) 804–14.
30. Banthia, N. Azzabi, M. & Pigeon, M., Restrained shrinkage cracking in fiber reinforced cementitious composites. *Materials and Structures RILEM (Paris)*, **26**(161) (1993) 405–13.

31. Banthia, N. & Dubeau, S., Steel and carbon micro-fiber reinforced cement-based materials for thin repairs. *ASCE Journal of Materials in Civil Engineering*, **6**(1) February (1994) 88–99.

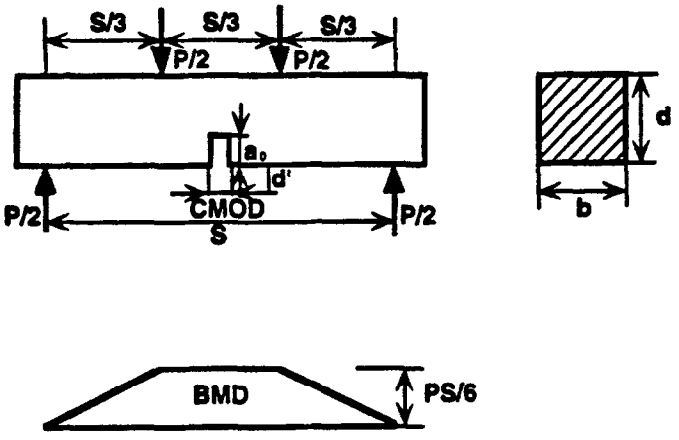

Fig. A.1

APPENDIX I

Let:

P =applied load.
S =span
b =width of the beam
d =depth of the beam
Δ =midspan displacement
CMOD =crack mouth opening displacement
CTOD =crack tip opening displacement
σ =flexural stress
a =crack length
a_o =initial crack (notch) length
a_{eff} =effective crack length ($>a_o$)
c =compliance=CMOD/P

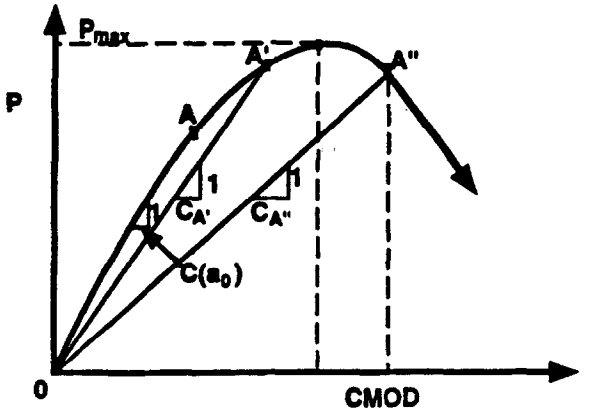

Fig. A.2

*Tada, H., Paris, P. C. and Irwin, G. R. *The Stress Analysis of Cracks Handbook*. Del Research Corp., Hellertown, PA, 1985.

$c(a_o)$ =initial compliance
$c(a_{eff})$ =compliance at a crack length a_{eff} $(>a_o)$
d' =depth from the bottom of the beam at which CMOD is measured

$$\alpha(a) = \left(\frac{a+d'}{d+d'}\right),\ \alpha(a_o)=\left(\frac{a_o+d'}{d+d'}\right),\ \alpha(a_{eff})=\left(\frac{a_{eff}+d'}{d+d'}\right)$$

M =moment

Effective crack length, a_{eff}

CMOD is given by*

$$\text{CMOD}=\frac{6\sigma a}{E}V_1(\alpha(a)) \tag{A1}$$

where

$$V_1[\alpha(a)]=0{\cdot}8-1{\cdot}7\alpha(a)+2{\cdot}4\alpha^2(a)+0{\cdot}66/(1-\alpha^2(a))$$

for a beam under third-point loading (Fig. A·1)

$$\sigma=\frac{PS}{bd^2} \tag{A2}$$

from (A1) and (A2)

$$E=4\left(\frac{P}{CMOD}\right)\left(\frac{aS}{bd^2}\right)(V_1(\alpha(a))) \tag{A3}$$

Writing eqn (A3) at the bend over point A and at any other point A′ or A″

$$E=\frac{4}{c(a_o)}\frac{a_oS}{bd^2}V_1[\alpha(a_o)]\Big|=\frac{4}{c(a_{eff})}\frac{a_{eff}S}{bd^2}V_1[\alpha(a_{eff})]\Big| \tag{A4}$$

at point A at points A′ or A″

from (A4)

$$a_{eff}\Big|=\frac{c(a_{eff})}{c(a_o)}\times a_o\left[\frac{V_1\alpha(a_o)}{V_1\alpha(a_{eff})}\right]$$

at points A′ or A″

Stress intensity factor*, $K_I(a)$

$$K_I(a)=\sigma\sqrt{\pi a}F_1\quad(a/d)$$

where

$$F_1(a/d)=1{\cdot}122-1{\cdot}40(a/d)+7{\cdot}33(a/d)^2-13{\cdot}08(a/d)^3+14{\cdot}0(a/d)^4$$

and σ is given by eqn (A2).

Crack tip opening displacement, CTOD

$$\text{CTOD}=\text{CMODZ}[\alpha(a),\beta(a)]$$

where

$$\alpha(a)=a/d,\beta(a)=a_o/a$$

and

$$Z[\alpha(a),\beta(a)]=[(1-\beta(a))^2+(1{\cdot}081-1{\cdot}49\alpha(a))(\beta(a)-\beta^2(a))]^{1/2}$$